Received: 31 October 2018 | Revised: 19 March 2019 | Accepted: 20 March 2019

DOI: 10.1002/sia.6649

RESEARCH ARTICLE

WILEY SURFACE and INTERFACE ANALYSIS

The influence of dielectric layer on the thermal boundary resistance of GaN-on-diamond substrate

Xin Jia[1] | Jun-jun Wei[1] | Yuechan Kong[2] | Cheng-ming Li[1] | Jinlong Liu[1] | Liangxian Chen[1] | Fangyuan Sun[3] | Xinwei Wang[4]

[1] Institute for Advanced Materials and Technology, University of Science and Technology Beijing, Beijing, China

[2] Science and Technology on Monolithic Integrated Circuits and Modules Laboratory, Nanjing Electronic Devices Institute, Nanjing, China

[3] Institute of Engineering Thermophysics, Chinese Academy of Sciences, Beijing, China

[4] College of Pipeline and Civil Engineering, China University of Petroleum (East China), Qingdao, China

Correspondence
Jun-jun Wei, Institute for Advanced Materials and Technology, University of Science and Technology Beijing, Beijing 100083, China.
Email: weijj@ustb.edu.cn

Funding information
European Union's Horizon 2020 Research and Innovation Staff Exchange (RISE) program, Grant/Award Number: 734578; National Key Research and Development Program of China, Grant/Award Number: 2018YFB0406500; Equipment Advanced Research Fund Project, Grant/Award Number: 614280301031704

The cooling behavior of GaN-on-diamond substrate can be enhanced by reducing the thermal boundary resistance (TBR), which is mainly determined by the nature of interlayer. Although SiN film is considered as the primary candidate of dielectric layer, it is still needed to be optimized. In order to facilitate the understanding of the influence of dielectric layer on the TBR of GaN-on-Diamond substrate, aluminum nitride (AlN), and silicon nitride (SiN) film were compared systematically, both of which are 100 nm. The time-domain thermoreflectance (TDTR) measurements, adhesion evaluation, and microstructural analysis methods were adopted to analyse these two interlayers. The results show the TBR of SiN interlayer is as low as 38.5 ± 2.4 $m^2K\ GW^{-1}$, comparing with the value of 56.4 ± 5.5 $m^2K\ GW^{-1}$ for AlN interlayer. The difference of TBR between these two interlayers is elucidated by the diamond nucleation density, and the adhesion between the diamond film and GaN substrate, both of which are affected by the surface charge and chemical groups of the dielectric layer.

KEYWORDS

AlN, dielectric layers, GaN-on-diamond, SiN, thermal boundary resistance, time-domain thermoreflectance

1 | INTRODUCTION

Gallium nitride (GaN) is an important semiconductor material, for example, GaN high-electron-mobility transistors (HEMTs).[1-3] Silicon carbide (SiC) has a high thermal conductivity (approximately 450 $W\ m^{-1}\ K^{-1}$), which makes it to be as a standard substrate material and provide decent heat spreading for GaN-based devices. However, with the further increasing power of GaN devices, the high heat flux generated makes the near-junction thermal management demand higher heat dissipation from the substrate material because heat removal near the junction becomes increasingly important for device performance and reliability. Chemical vapor deposited (CVD) polycrystalline diamond has the highest thermal conductivity reaching up to 2000 $W\ m^{-1}\ K^{-1}$, which can greatly improve the thermal management of a GaN device.[4] The GaN-on-diamond shows an increase in three times the power density and lower junction temperatures than those on a GaN-on-SiC device.[5-10]

However, for a GaN-on-diamond device, the heat spreading capability is dependent on not only the diamond thermal conductivity but also the significant effective thermal boundary resistance (TBR) of the GaN/diamond interface. TBR is a lump resistance, including contributions to a dielectric layer and the high-grain-boundary-density diamond near to the interface. A dielectric layer is usually used to protect the GaN and to evenly deposit diamond seeds.[11] To reduce the TBR between the diamond and the GaN, the grain size of the diamond crystallites can be adjusted to be as close as possible near the nucleation region for maximum thermal conductivity,[12] and the dielectric layer used to seed the diamond can be made as thin as possible and minimizing thermal resistance.[7] In addition, the nucleation density of the grown diamond affecting the integrity and adhesion capability

of the GaN/diamond interface is also very important to the TBR, while the influence of such nucleation on TBR is not elucidated clearly.

In this work, the TBR of GaN-on-diamond wafers fabricated from different dielectric layers were studied by using a recently developed fully contactless transient thermoreflectance technique. The analysis of material structures, adhesive force, characteristic interface features, nucleation density, micro scratch testing, and atomic force microscope (AFM) were used to explain the mechanism of influence of different dielectric layers on TBR, respectively. It demonstrated that the TBR of GaN-on-diamond wafers could be optimized significantly if high nucleation density was obtained before diamond film growth.

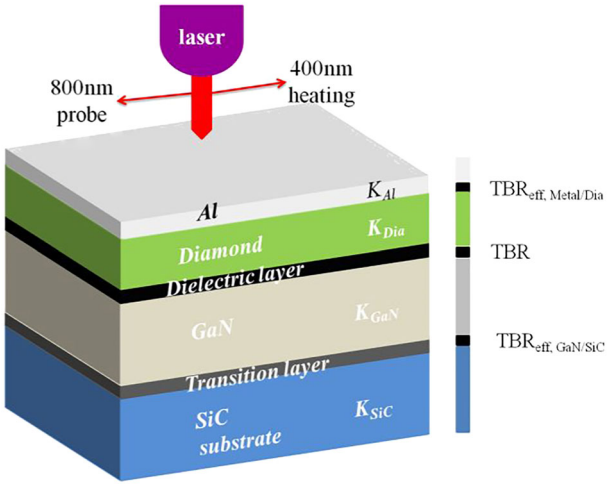

FIGURE 1 Sample structure and time-domain thermoreflectance measurement scheme

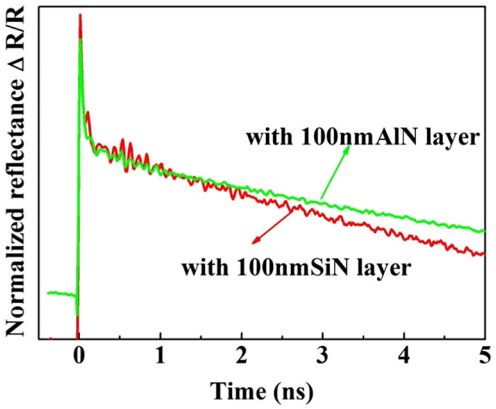

FIGURE 2 Normalized thermoreflectance signal as a function of time of GaN-on-diamond samples for different dielectric layers of SiN and AlN dielectric layers between diamond and GaN

2 | EXPERIMENTAL DETAILS

GaN-on-SiC was used as the substrate and bought from Nanjing Electronic Devices Institute, China. To protect GaN surfaces against an abrasion and plasma chemical vapor deposition (CVD) environment, a SiN and AlN dielectric layer with a thickness of 100 nm was deposited, respectively, by using radio frequency (RF) magnetron sputtering. The nano-diamond (ND) seeding was performed by using sample immersion into an aqueous nano-diamond colloid for a few seconds, followed by deionized water rinsing in deionized water and drying using a spin coater. The size of the hydrogen-annealed NDs was 30 nm with a zeta-potential of approximately +80 mV, PH approximately 5-6. After that, an approximately 2-μm thick polycrystalline diamond layer was grown on the GaN surface by a homemade microwave plasma CVD system.

The surface morphology of the GaN-on-diamond structure was observed through a scanning electron microscope (SEM) (ZEISS EVO 18). The adhesion force between the diamond film and the GaN substrate was evaluated by a micro scratch tester (WS-2005). A calculation of a seeding density *N* was attempted by analyzing the AFM images, as well as SEM micrograph. The surface chemical state of the dielectric layer was determined using X-ray photoelectron spectroscopy (XPS).

To evaluate the thermal properties of the Diamond/Interlayer/GaN structure, a transient thermal reflection technique was used. Before thermal testing, a 100-nm thick aluminum film was deposited on the diamond surface by an e-beam evaporation method to serve not only as a transducer layer but also as a sensor layer for absorbing the energy from the pump laser. The absorption is then converted to heat, indicating the temperature of the sample surface via the thermoreflectance effect.[13] The sample structure and the TDTR measurement principle are illustrated in Figure 1. A heating pulse from a 400-nm frequency doubled Ti: Sapphire laser was absorbed into the aluminum, with the laser emitting a pulse duration and a pulse frequency of 200 fs and 80 MHz, respectively. The surface reflectance of the aluminum film was probed by an 800-nm frequency-doubled Ti: Sapphire laser to track the temperature rise. In addition, the heating and probe laser spot sizes were 30 μm and 15 μm, respectively. More details of the technique are described in Sun et al.[13]

3 | RESULTS AND DISCUSSION

Figure 2 shows the normalized reflectance transients of two structures of different dielectric layer measured at room temperature. The values of $G_{Al/dia}$ ($TBR_{Al/dia}$) approximately 20 $m^2K\ GW^{-1}$ and

TABLE 1 Fixed input thermal parameters for different materials in the GaN-on-diamond samples

Layer	Al	Diamond	GaN	SiC
Thickness, nm	100	2000	2000	500 000
Thermal conductivity, W/mK	237	Fitted	130	460
Specific heat, J/kgK	896	500	430	690
Density, kg/m^3	2700	3500	6150	2320

$G_{GaN/SiC}$ ($TBR_{GaN/SiC}$) approximately 30 $m^2K\ GW^{-1}$ were measured before. The thermal physical parameters of each layer for the analytical data of TDTR are shown in Table 1. The sensitivity analysis results of each parameter were shown in Figure 3. It can be seen that the sensitivity of $G_{Dia/GaN}$ ($TBR_{dia/GaN}$) and k_{dia} is significantly greater than other parameters. It shows that this structure can obtain more accurate $G_{Dia/GaN}$ through the amplitude signal of TDTR. In addition, the sensitivity of k_{dia} is the largest, which means that the accuracy of k_{dia} has a great influence on the accuracy of the $G_{Dia/GaN}$ test value, and the influence of other parameters is small. This also means that if any of the $G_{dia/GaN}$ values are adapted to our measurement data, the amplitude sensitivity of $G_{dia/GaN}$ and k_{dia} does not change much. A more detailed analysis of the sensitivity is reflected in the Zhou Y.[11] Table 2 shows the extracted $TBR_{eff,\ Dia/GaN}$ for different barrier layers under the same preparation conditions. The TBR of the GaN/diamond with the SiN dielectric layer is 38.5 ± 2.4 $m^2K\ GW^{-1}$, and with the AlN dielectric layer is 56.4 ± 5.5 $m^2K\ GW^{-1}$, respectively. This is similar to the results of Sun Het, whose result is 50 ± 5 $m^2K\ GW^{-1}$. And they reduced the TBR to 12 $m^2K\ GW^{-1}$ by reducing the thickness of the SiN layer and the thickness of the diamond nucleation layer. However, Zhou Y[11] reports that the TBR are approximately 10 $m^2K\ GW^{-1}$ and approximately (12-64) $m^2K\ GW^{-1}$, and using 5-nm thick SiN and AlN as the dielectric layer, respectively. They believe that the TBR of AlN as the dielectric layer is very high because a rougher interface with a step-shaped microstructure is formed into the diamond/GaN interfaces. In addition, they believe that approximately 60 nm of GaN has been etched away because of lack of protection from the harsh diamond growth environment, and the diamond nucleation layer was thicker. Although the TBR results are similar to those in the literature, there are probably other factors that affect TBR for different dielectric layer types with the same thickness.

Apparently, the thermal conductivity of the dielectric layer is an important factor affecting the TBR. The literature[14]shows that the crystalline Si_3N_4 has a thermal conductivity of 30 $Wm^{-1}\ K^{-1}$. However, for thin amorphous SiN, much lower values are reported.[15] Typically, the thermal conductivity of the SiN layer[16] is approximately 1 $Wm^{-1}\ K^{-1}$. The thermal conductivity of AlN[17] can theoretically be achieved at 320 $Wm^{-1}\ K^{-1}$. Similarly, the thermal conductivity of AlN films is as low as approximately 15 $Wm^{-1}\ K^{-1}$ once the AlN film is less than 400 nm,[18] which it is still much higher than the SiN film. Therefore, theoretically, the thermal conductivity of the AlN interlayer is greater than the thermal conductivity of the SiN interlayer. In other words, in theory, the TBR of the diamond/AlN/GaN structure should be lower than the structure with SiN interlayer. Unfortunately, in our study, the TBR of the diamond/SiN/GaN structure is even lower than the TBR of the diamond/AlN/GaN structure. Usually, TBR originated from the dielectric layer itself, and the initial nucleation layer of diamond growth. As a result, even though the thermal conductivity of AlN interlayer is much higher than that of SiN, the nucleation layer probably play a more crucial role on the TBR.

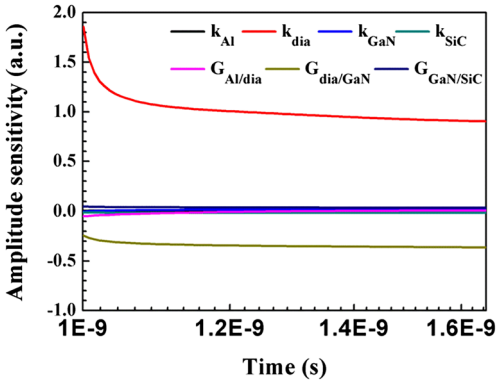

FIGURE 3 Sensitivity analysis of time-domain thermoreflectance (TDTR) signals for GaN-SiN-diamond samples

A calculation of seeding density *N* was attempted by analyzing the AFM images after NDs seeding (Figure 4) on the dielectric layers. In the case of the SiN dielectric layer, the NDs seeds density *(N)* is about 7.5 × 10^{11} cm^{-2}, which is estimated by the attachment software (image analysis) of AFM. And if the AlN film is as the dielectric layer, a few ND seeds are visible, and *N*~1.2 × 10^{10} cm^{-2} is estimated. To confirm these calculations, the seeded samples were exposed to 12% CH_4:H_2:(0.3%)N_2 plasma in an MPG-2050C series MPCVD reactor with a total pressure of 60 torr, a substrate temperature of 800°C, and a microwave power of 1000 W. The diamond growth was initiated for 5 minutes to enlarge the ND seeds in order to facilitate the calculation of ND seeding density.

After a short nucleation treatment, we stop the MPCVD system, and observe the surface by SEM (Figure 5). The diamond nucleation cores on the surface are assumed mainly from the attached NDs before, so that we can speculate the seeding density by calculating the nucleation density basing on the SEM morphology. As a result, the ND seeding density achieved on AlN surfaces was 1.2 × 10^{10} cm^{-2}, whereas on SiN surface, the density reaches 1 × 10^{12} cm^{-2}, which is very close to the estimated result from the AFM image, and consistent to other references reported.[19-21] This result also can verify the assumption that the ND seeding is the dominated pretreatment method to enhance the diamond nucleation, as well as the density film deposition.

In order to eliminate the influence of roughness of the dielectric layer on the seeding density, we measured the roughness of the SiN and AlN intermediate layers before seeding. The Ra of SiN was 0.8 nm, while the Ra of AlN was 0.6 nm (as shown in Figure 6A). It is generally believed that the effect of similar roughness on seeding density should be similar, and the ND particles adhesion of the two

TABLE 2 Fit model results of thermal boundary resistance (TBR) of two structures

Structure	Dielectric Layers Thickness	Diamond Nucleation Time (12% CH_4)	Grow Time (5% CH_4)	TBR ($m^2K\ GW^{-1}$)
Diamond/SiN/GaN	100 nm SiN	15 min	120 min	38.5 ± 2.4
Diamond/AlN/GaN	100 nm AlN			56.4 ± 5.5

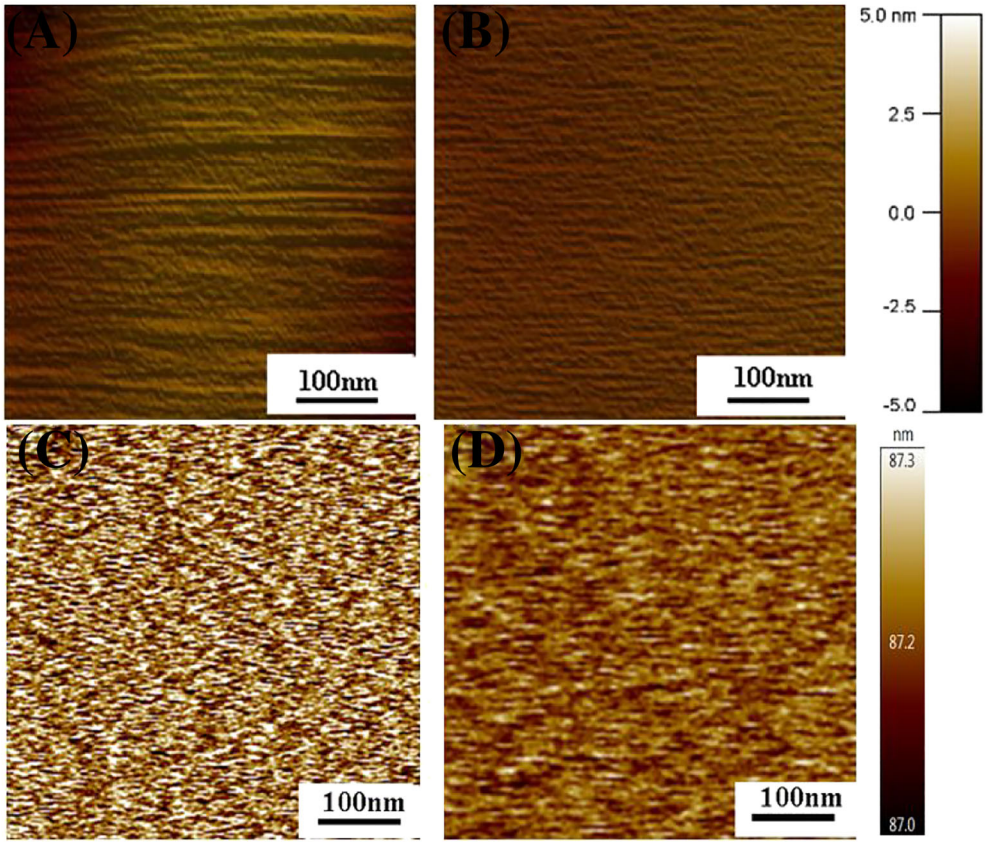

FIGURE 4 Atomic force microscope (AFM) of A, untreated SiN dielectric layer Ra = 0.8 nm and B, untreated AlN dielectric layer Ra = 0.6 nm, C, after nano-diamond (ND) seeding SiN dielectric layer and D, after ND seeding AlN dielectric layer

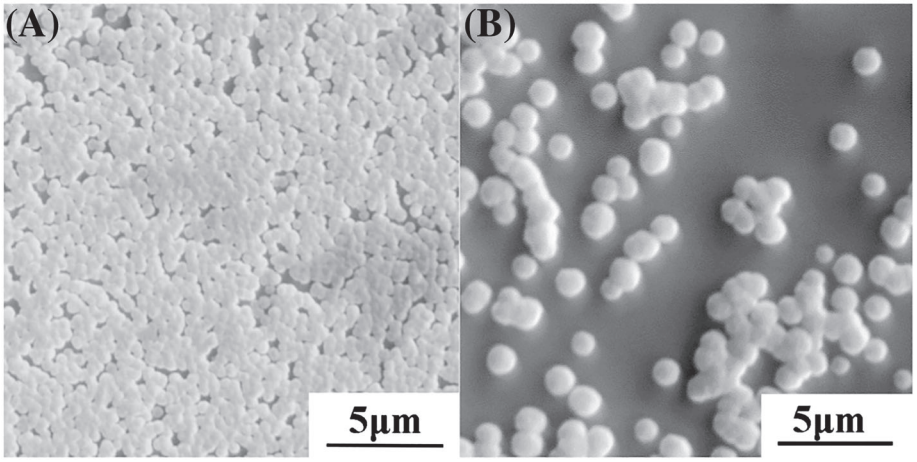

FIGURE 5 Scanning electron microscope (SEM) images after 5 minutes diamond nucleation on the dielectric layer of SiN dielectric layer A, and AlN dielectric layer B

dielectric layers should be similar. Here, the surface chemical state of the dielectric layer probably dominate the surface seeding process, and then finally affect the diamond nucleation density.

Oliver A. Williams[20] reports that the Ga-face and N-face of GaN have a different polarity and potential, which have different effects on nano-diamond powders of different terminals and have a great influence on the seeding density. In addition, the growth of diamond on GaN was carried out on both Ga and N-face of GaN. But in this study, the dielectric layer is deposited on the top side of GaN. The dielectric layer avoids the existence of different polarity faces of GaN, and it is also more convenient to analyze the influence of dielectric layer on seeding.

XPS is adopted to analyze the surface chemical state of both interlayers, and the results are shown in Figure 6. As a binding-energy

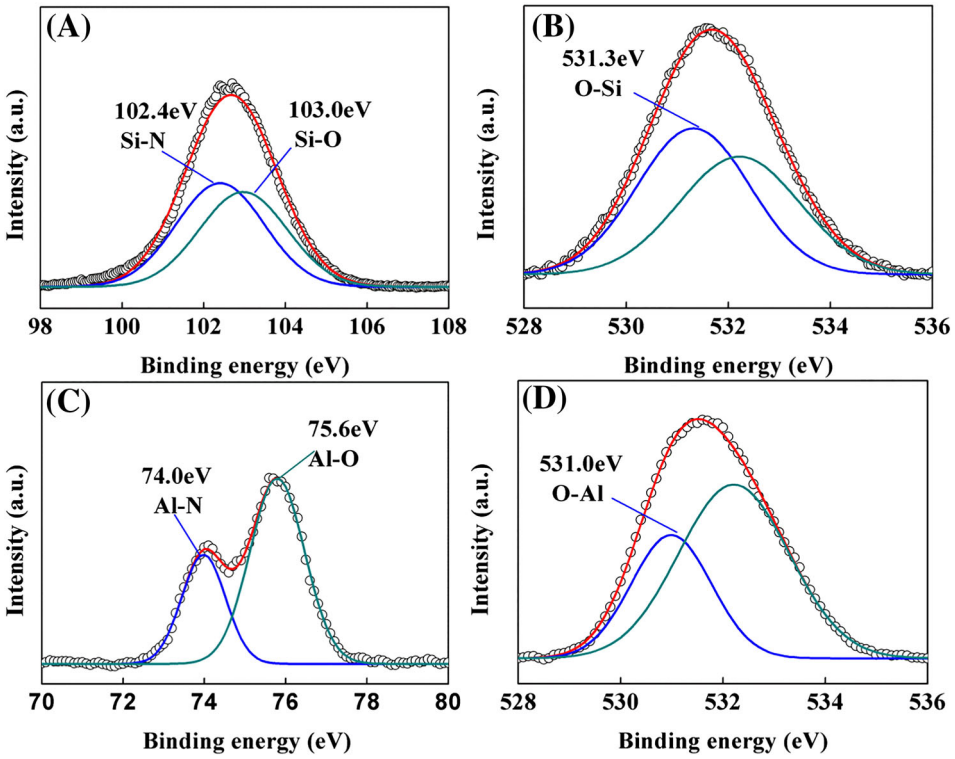

FIGURE 6 X-ray photoelectron spectroscopy (XPS) spectra and peak fitting of Si_{2P} peak A, and O_{1s} B, of the SiN film, Al_{2p} peak C, and O_{1s} D, of the AlN film

reference, the primary C_{1s} peak for adventitious surface carbon was set at 284.8 eV. According to the XPS results, the Al_{2p} core-level binding energy is 74.0 eV and 75.6 eV, respectively, which matches the value reported for wurtzite AlN.[17] The Al_{2p} photoelectron peak shifts of 74.0 eV is Al—N bonds, since the Al_{2p} photoelectron peak shifts toward a higher binding energy, 75.6 eV. This result indicates the presence of Al—O bonds probably resulting in the formation of Al_2O_3.[22] Meanwhile, the O_{1s} core-level binding energy is 531.0 eV, the result means the presence of O—Al bonds. The impurity oxygen is unavoidable in the process of sputtering AlN dielectric layer so that the surface of AlN films is likely to be covered with surface oxide groups.[23]

To explain the observation of low ND seeding density on the AlN dielectric layer, the surface functional groups and the zeta potential of the NDs colloid was introduced. The used ND-seed colloid is water-based, possesses positive zeta-potential and has a faintly acid PH. This situation implies that acidic groups (eg, R–COOH and R–OH) are present on the surface of the ND particles.[24] When the AlN dielectric layer is immersed into the water-based colloidal solution, the surface rapidly hydrolyzes by forming AlOOH and/or Al $(OH)_3$ in an exothermic reaction.[25,26] In addition, because of the presence of Al—O bonds, the surface of the AlN dielectric layer will form several kinds of several compounds in the aqueous environment, e.g. Al_3OH, Al_2OH, and $AlOH_2$.[27] A majority of Al—OH groups on the surface lead to a positive zeta potential in an aqueous environment since Al—OH groups accept protons or release OH^- ions.[28] These hydroxyl groups form a positively charged surface at PH 3-8, causing the repulsion of the ND seeds, which is also positively charged measured by Zeta potential. More —OH groups cause the surface move positive charge, which leads to the less NDs attachment. As a result, the number of NDs attached to the AlN dielectric layer surface is limited, which will induce the low diamond nucleation density consequently. This mutual repulsion process as illustrated in Figure 7.

In contrast, this repulsion does not occur on the surface of the SiN dielectric layer. According to the XPS results shown in Figure 6A and 6B, the Si_{2P} core-level binding energy is divided into 102.4 eV and 103.0 eV, which attributes to the Si—N bond and the Si—O bond. Similar to AlN's XPS results, the O_{1s} core-level binding energy is 531.3 eV, the result means that the presence of O—Si bonds. The Si—O bond is also from the surface absorption reaction with O_2 or H_2O when sample is exposed to the aqueous environment. Further absorption of

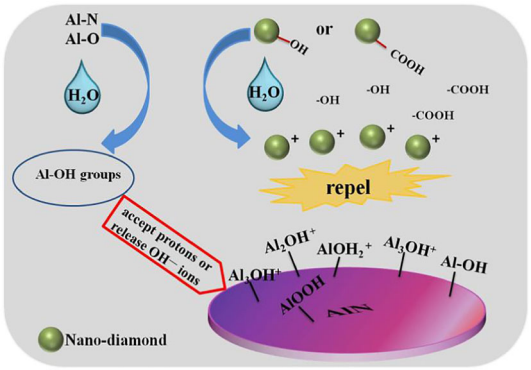

FIGURE 7 Schematic diagram of mutual repulsion between AlN dielectric layer and nano-diamonds (NDs) in the aqueous environment

H_2O will induce the formation of $(OH)_3SiO^-$ ions on the SiN surface.[29-32] Therefore, A majority of negative potential $(OH)_3SiO^-$ groups on the SiN surface dramatically improve the attraction of NDs on the SiN dielectric layer surface, it is the main driving force for nanodiamond self-assembly. And subsequently enhance the diamond nucleation density.

The TBR is also partially affected by the disordered layer in the near-interface diamond layer. The near-interface diamond thermal conductivity is controlled by the quality of the nucleation layer. The lower nucleation density probably increases the number of holes and defects, which will increase the thermal resistance. Obviously, the thermal conductivity of nucleation layer is significantly lower than that of good crystalline film because of phonon scattering at grain boundaries and point defects and holes.[33,34] The lower nucleation density makes it difficult to form a dense diamond film in a short time. Instead, the thickness of the nucleation layer is increased, which then negatively impacts its thermal conductivity.

The excellent adhesion between diamond film and the substrate further reduce the TBR. To assess the adhesion of the diamond film on GaN, a micro scratch test was implemented after growing the diamond film on GaN by MPCVD. The test has already been used by a number of groups to study hard, thin, and well-adhering coatings.[35,36] More detail on the method are described in Nakao et al.[35] In addition, the nanoindentation method is also a very common quantitative, semi-quantitative method for measuring the adhesion energy properties of coating/substrate materials, such as Dong Liu[37] and Q. Zhou et al.[38] The change of acoustic signal for brittle diamond film on the GaN substrate reflects this adhesion, as shown in Figure 8. The acoustic signal shows that the critical load of the GaN-SiN-Diamond sample is 14 N. While the critical load of the GaN-AlN-Diamond sample is only about 6 N. The results shows that the diamond film on the GaN with the AlN dielectric layer has a lower adhesion compared with the sample with the SiN dielectric layer and proper selection of the dielectric layer can improve the adhesion of the film.[39] The high adhesion on SiN interlayer is originated from not only the higher nucleation density of the ND particles to the surface, but also the better interface microstructure. As to the Si-rich structure in amorphous SiN dielectric layers, perhaps a few nanometers thick Si-rich SiN layer may convert to Si-C before diamond nucleation. In Figure 9, the interface is smooth and the elements are distributed an orderly transition. It was also found through high-resolution imaging and EDS analysis that a relatively smooth and ordered elemental transition happens throughout the interlayer, thereby reducing disorder and enhancing phonon transport across the interface.[40] In addition, because there are a small mismatch of lattice constant as well as thermal expansion coefficient between SiC(4.8×10^{-6}/°C) and GaN(5.6×10^{-6}/°C), SiC and the diamond film can form strong chemical bonding, which could contribute to a good adhesion of the deposited diamond on the GaN substrate finally. Therefore, because of the aforementioned favorable conditions, the TBR is lower when SiN film is the dielectric layer.

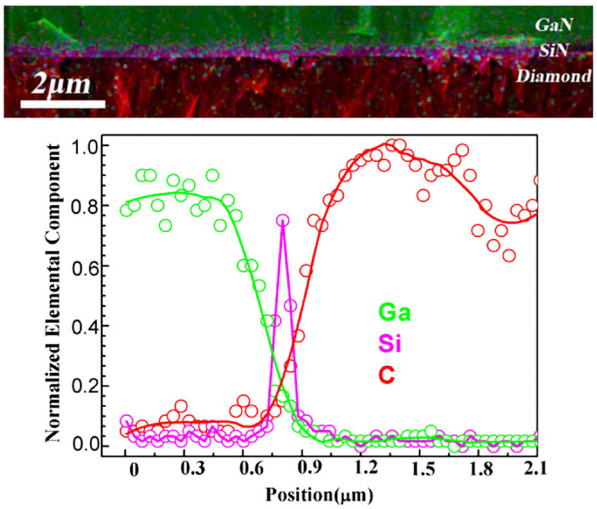

FIGURE 9 (Top) composition mapping of an energy-dispersive X-ray spectroscopy (EDS) map scan across the GaN/diamond interface, (bottom) averaged intensity along the long direction in (top) showing the elemental components of each section

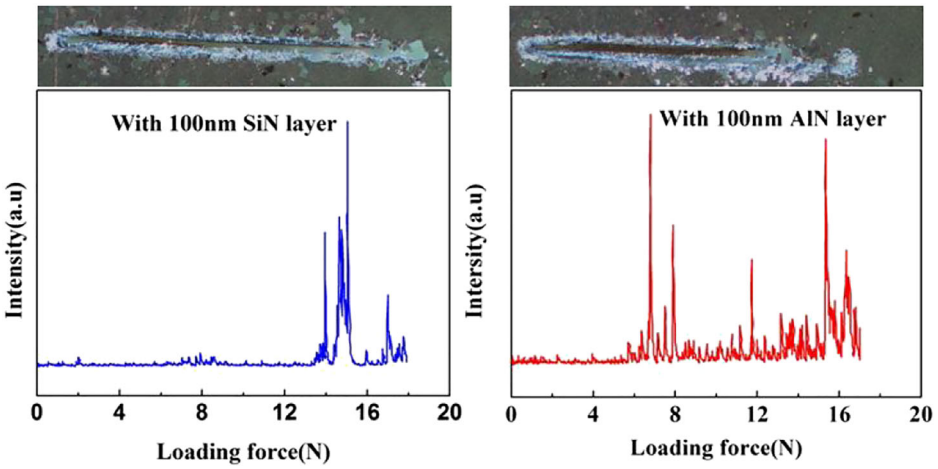

FIGURE 8 Sound signal and corresponding scratch morphology of diamond film on the GaN substrate with different dielectric layers

4 | CONCLUSIONS

In this study, the AlN and SiN interlayer were adopted as the dielectric layers for growing diamond on GaN substrate, respectively. A time-domain thermoreflectance study revealed the TBR of both structures as well. The NDs seeding and the following nucleation are considered as the important influence factors on the TBR. The structure with SiN dielectric layer shows a lower TBR than that with AlN dielectric layer, which can be explained by the high efficiency of NDs seeding on SiN surface. Because of the positive zeta potential and oxygen absorption on the AlN surface, NDs are strongly repelled on the surface resulting in a low NDs density about 1.2×10^{10} cm^{-2}. In contrast, the NDs attachment is enhanced due to the negative potential of the SiN dielectric layer surface. This enhancement can obviously facilitate diamond nucleation and diamond growth on SiN interlayer. In addition, Si—C bonding during diamond nucleation is also beneficial to the strong film adhesion and low TBR.

In conclusion, high NDs seeding density and strong diamond film adhesion on the dielectric layer are the dominated factors to affect the TBR between diamond film and GaN substrate. It can be speculated that a selected modification for the surface chemical state of dielectric layer would be a promising option to obtain the TBR as low as possible.

ACKNOWLEDGEMENTS

Different aspects of this work were partially supported by National Key Research and Development Program of China (grant No. 2018YFB0406500) Equipment Advanced Research Fund Project (grant No. 614280301031704) and European Union's Horizon 2020 Research and Innovation Staff Exchange (RISE) program (grant No. 734578).

ORCID

Xin Jia https://orcid.org/0000-0003-1211-6679
Jun-jun Wei https://orcid.org/0000-0002-4245-2289

REFERENCES

1. Dora Y, Chakraborty A, McCarthy L, et al. High breakdown voltage achieved on AlGaN/GaN HEMTs with integrated slant field plates. *IEEE Electron Device Lett*. 2006;27(9):713-715.
2. Brown JD, Gibb S, McKenna J, et al. Performance, reliability, and manufacturability of AlGaN/GaN high electron mobility transistors on silicon carbide substrates. *ECS Trans*. 2006;3(5):161-179.
3. Mishra UK, Shen L, Kazior TE, et al. GaN-based RF power devices and amplifiers. *Proc IEEE*. 2008;96(2):287-305.
4. Francis D, Faili F, Babić D, Ejeckam F, Nurmikko A, Maris H. Formation and characterization of 4-inch GaN-on-diamond substrates. *Diamond Relat Mater*. 2010;19(2-3):229-233.
5. Dumka DC, Chou TM, Faili F, et al. AlGaN/GaN HEMTs on diamond substrate with over 7 W/mm output power density at 10 GHz. *Electron Lett*. 2013;49(20):1298-1299.
6. Pomeroy JW, Bernardoni M, Dumka DC, Fanning DM, Kuball M. Low thermal resistance GaN-on-diamond transistors characterized by three-dimensional Raman thermography mapping. *Appl Phys Lett*. 2014;104(8):083513.
7. Sun H, Simon RB, Pomeroy JW, et al. Reducing GaN-on-diamond interfacial thermal resistance for high power transistor applications. *Appl Phys Lett*. 2015;106(11):111906.
8. Chao PC, Chu K, Creamer C, et al. Low-temperature bonded GaN-on-diamond HEMTs with 11 W/mm output power at 10 GHz. *IEEE Trans Electron Devices*. 2015;62(11):3658-3664.
9. Altman D, Tyhach M, McClymonds J, et al. Analysis and characterization of thermal transport in GaN HEMTs on diamond substrates. 2014 IEEE intersociety conference on. IEEE, 2014.
10. Pomeroy JW, Simon RB, Sun H, et al. Contactless thermal boundary resistance measurement of GaN-on-diamond wafers. *IEEE Electron Device Lett*. 2014;35(10):1007-1009.
11. Zhou Y, Anaya J, Pomeroy J, et al. Barrier-layer optimization for enhanced GaN-on-diamond device cooling. *ACS Appl Mater Interfaces*. 2017;9(39):34416-34422.
12. Anaya J, Rossi S, Alomari M, et al. Control of the in-plane thermal conductivity of ultra-thin nanocrystalline diamond films through the grain and grain boundary properties. *Acta Mater*. 2016;103:141-152.
13. Sun F, Wang X, Yang M, et al. Simultaneous measurement of thermal conductivity and specific heat in a single TDTR experiment. *Int J Thermophys*. 2018;39(1):5.
14. Seelmann-Eggebert M, Meisen P, Schaudel F, Koidl P, Vescan A, Leier H. Heat-spreading diamond films for GaN-based high-power transistor devices. *Diamond Relat Mater*. 2001;10(3–7):744-749.
15. Mirmira SR, Fletcher LS. Review of the thermal conductivity of thin films. *J Thermophys Heat Transfer*. 1998;12(2):121-131.
16. Cho J, Francis D, Altman DH, Asheghi M, Goodson KE. Phonon conduction in GaN-diamond composite substrates. *J Appl Phys*. 2017;121(5):055105.
17. Slack GA, Tanzilli RA, Pohl RO, Vandersande JW. The intrinsic thermal conductivity of AlN. *J Phys Chem Solid*. 1987;48(7):641-647.
18. Zhao Y, Zhu C, Wang S, et al. Pulsed photothermal reflectance measurement of the thermal conductivity of sputtered aluminum nitride thin films. *J Appl Phys*. 2004;96(8):4563-4568.
19. Pobedinskas P, Degutis G, Dexters W, et al. Surface plasma pretreatment for enhanced diamond nucleation on AlN. *Appl Phys Lett*. 2013;102(20):201609.
20. Mandal S, Thomas ELH, Middleton C, et al. Surface zeta potential and diamond seeding on gallium nitride films. *ACS Omega*. 2017;2(10):7275-7280.
21. Liu D, Francis D, Faili F, et al. Impact of diamond seeding on the microstructural properties and thermal stability of GaN-on-diamond wafers for high-power electronic devices. *Scr Mater*. 2017;128:57-60.
22. Rosenberger L, Baird R, McCullen E, Auner G, Shreve G. XPS analysis of aluminum nitride films deposited by plasma source molecular beam epitaxy. *Surf Interface Anal*. 2008;40(9):1254-1261.
23. Dalmau R, Collazo R, Mita S, Sitar Z. X-ray photoelectron spectroscopy characterization of aluminum nitride surface oxides: thermal and hydrothermal evolution. *J Electron Mater*. 2007;36(4):414-419.
24. Boehm HP. Some aspects of the surface chemistry of carbon blacks and other carbons. *Carbon*. 1994;32(5):759-769.
25. Graziani T, Bellosi A. Degradation of dense AlN materials in aqueous environments. *Mater Chem Phys*. 1993;35(1):43-48.
26. Bowen P, Highfield JG, Mocellin A, Ring TA. Degradation of aluminum nitride powder in an aqueous environment. *J Am Ceram Soc*. 1990;73(3):724-728.

27. Sung J, Shen YR, Waychunas GA. The interfacial structure of water/protonated α-Al2O3 (11-20) as a function of pH. *J Phys Condens Matter*. 2012;24(12):124101.
28. Krnel K, Kosmac T. Reactivity of aluminum nitride powder in dilute inorganic acids. *J Am Ceram Soc*. 2000;83(6):1375-1378.
29. Raider SI, Flitsch R, Aboaf JA, et al. Surface oxidation of silicon nitride films. *J Electrochem Soc*. 1976;123(4):560-565.
30. Alexander GB, Heston WM, Iler RK. The solubility of amorphous silica in water. *J Phys Chem*. 1954;58(6):453-455.
31. Osenbach JW, Knolle WR. Behavior of a-SiN: H and a-SiON: H films in condensed water. *J Electrochem Soc*. 1992;139(11):3346-3351.
32. Vogt M, Hauptmann R. Plasma-deposited passivation layers for moisture and water protection. *Surf Coat Technol*. 1995;74:676-681.
33. Onn DG, Witek A, Qiu YZ, Anthony TR, Banholzer WF. Some aspects of the thermal conductivity of isotopically enriched diamond single crystals. *Phys Rev Lett*. 1992;68(18):2806-2809.
34. Zhu RH, Miao JY, Liu JL, et al. High temperature thermal conductivity of free-standing diamond films prepared by DC arc plasma jet CVD. *Diamond Relat Mater*. 2014;50:55-59.
35. Nakao S, Kim J, Choi J, Miyagawa S, Miyagawa Y, Ikeyama M. Micro-scratch test of DLC films on Si substrates prepared by bipolar-type plasma based ion implantation. *Surf Coat Technol*. 2007;201(19–20):8334-8338.
36. Chen S, Ma G, Wang H, He PF, Wang HM, Liu M. Evaluation of adhesion strength between amorphous splat and substrate by micro scratch method. *Surf Coat Technol*. 2018;344:43-51.
37. Liu D, Fabes S, Li B, et al. On the characterisation of the interfacial toughness in a novel "GaN-on-Diamond" material for high-power RF devices. *ACS Appl Electron Mater*. 2019;1(3):354-369.
38. Zhou Q, Ren Y, Du Y, et al. Adhesion energy and related plastic deformation mechanism of Cu/Ru nanostructured multilayer film. *J Alloys Compd*. 2019;772:823-827.
39. Chao X. Effects of pretreatment on quality and adhesion of diamond films on cemented carbides. *Surface Technol*. 2018. https://doi.org/10.16490/j.cnki.issn.1001-3660.2018.01.032
40. Yates L, Anderson J, Gu X, et al. Low thermal boundary resistance interfaces for GaN-on-diamond devices. *ACS Appl Mater Interfaces*. 2018;10(28):24302-24309.

How to cite this article: Jia X, Wei J, Kong Y, et al. The influence of dielectric layer on the thermal boundary resistance of GaN-on-diamond substrate. *Surf Interface Anal*. 2019;1–8. https://doi.org/10.1002/sia.6649